The Photo-Thermal Effect of Green-Synthesized Gold Nanoparticles on Human Breast Cancer Cells

Mpho Mohlongo[1], Blassan P. George[1], and Heidi Abrahamse[1*]

[1]Laser Research Centre, Faculty of Health Sciences, University of Johannesburg, P.O. Box 17011, Doornfontein 2028, South Africa

E-mail: habrahamse@uj.ac.za

Abstract. Breast cancer continues to be one of the main causes of cancer-related deaths among women globally, highlighting the need for new, targeted, and less harmful treatment options. Gold nanoparticles have been identified as potential tools in nanomedicine due to their compatibility with biological systems, customizable surface chemistry, and distinctive optical characteristics. Nevertheless, traditional synthesis methods often utilize toxic reducing agents, which limit their use in medicine. This study investigates an environmentally friendly method for synthesizing gold nanoparticles using an extract from the *Kniphofia porphyrantha* plant and assesses their effectiveness in treating breast cancer. The gold nanoparticles were synthesized by utilizing extracts of the plant that function as both reducing agents and stabilizing agents. The spectrophotometric analysis was performed to confirm the optical properties of gold nanoparticles, while phototoxic effects of synthesized gold nanoparticles on MCF-7 breast cancer cells were evaluated by assessing morphological changes, cellular viability, and cytotoxicity rates 24 hours post-irradiation using a 525 nm laser with a fluency of 10 J/cm^2. Results showed a dose-dependent response to the treatment, demonstrated by significant morphological changes, increased cytotoxicity, and decreased cell viability compared to untreated cells, indicating the anticancer properties of green-synthesized gold nanoparticles. This highlights the dual advantages of plant-based gold nanoparticles: sustainable production and potential use in cancer therapy. These results encourage further exploration of the optical properties and biological activity of plant-based gold nanoparticles as promising candidates for cancer nanomedicine.

1 Introduction

Female breast cancer remains the predominant cause of cancer-associated mortality among women globally. It was the second most commonly diagnosed cancer in 2022, with an estimated 2.3 million cases and approximately 660 000 deaths, accounting for 11.6% of all cancer cases and 6.9% of all cancer-related deaths [1, 2]. Current therapeutic strategies face significant limitations, including systemic toxicity, drug resistance, and non-specific targeting of healthy tissues. These challenges necessitate the development of innovative treatment modalities with enhanced specificity and reduced off-target effects [3, 4]. Photothermal therapy (PTT) has emerged as a promising non-invasive approach for selective tumour damage. This technique exploits the principle that cancer cells exhibit heightened sensitivity to hyperthermic conditions (41-48°C) compared to healthy tissues. When exposed to visible or near-infrared light (NIR), photothermal agents generate localized heat that induces protein denaturation, membrane disruption, and ultimately selective tumor cell necrosis [3, 5].

Gold nanoparticles (AuNPs) have gained substantial attention as ideal PTT agents due to their exceptional localized surface plasmon resonance (LSPR) properties. Key advantages include tuneable optical properties, enhanced thermal conversion, and passive tumour targeting. Conventional synthesis methods, however, frequently employ cytotoxic reduction agents (such as sodium borohydride) that compromise biocompatibility and necessitate extensive purification. Plant-meditated synthesis offers a sustainable alternative by utilizing phytochemicals as both reducing and stabilizing agents [3]. *Kniphophia porphyrantha*, a South African indigenous plant, contains abundant flavonoids and phenolic acids [6] that facilitate nanoparticle formation while potentially enhancing therapeutic efficacy [3, 7]. This study establishes a green synthesis protocol for AuNPs using *K. porphyrantha* extract and evaluates their optical properties relevant to PTT applications, photothermal cytotoxicity against MCF-7 breast cancer cells, and dose-dependent therapeutic response under laser irradiation.

2 Methodology

2.1 Preparation of plant extract and synthesis of gold nanoparticles

Healthy leaves of K. porphyrantha were sun-dried and finely powdered. Approximately 10 g of the powdered plant materials were mixed with 100 mL of methanol and boiled for 48 hours. at 55°C and 100 rpm. After cooling to room temperature, the mixture was filtered using a 0.22 µm syringe filter to obtain the extract used for nanoparticle synthesis. For green synthesis of AuNPs, 10 mL of plant extract was added to 50 mL of 0.1 mM aqueous chloroauric acid ($HAuCl_4$) solution. The reaction mixture was placed on a magnetic hot plate stirrer for 20 mins at 90°C and 100 rpm, followed by centrifugation at 18 000 rm for 15 mins. The resulting pellet was washed with deionized water and stored for further characterization and biological evaluation.

2.2 Characterization of gold nanoparticles

The green synthesized AuNPs were characterized using various analytical techniques:

2.2.1 UV-vis spectrometry to determine optical properties. Absorbance spectra were recorded between 300 and 800 nm to confirm the formation of AuNPs through surface plasmon resonance (SPR), typically peaking around 520 nm.

2.2.2 Size distribution and Zeta potential. Dynamic light scattering (DLS) and Zeta potential (ZP) were performed using the Malvern Zeta Sizer Nano series. DLS was used to measure the hydrodynamic diameter and particles size distribution to assess colloidal uniformity. ZP was used to evaluate the surface charge and predict colloidal stability.

2.3 Cell culture and treatment of experimental groups

The human breast adenocarcinoma MCF-7 (ATTC® HTB-22) cell line was maintained as monolayers in T75 flasks using Dulbecco's Modified Eagle Medium (DMEM) supplemented with 10% fetal bovine serum (FBS), 1% amphotericin B, and 1% penicillin-streptomycin. Cells were incubated at 37°C in a humidified atmosphere of 95% air and 5% CO_2. For experiments, cells were seeded at 200 x 10^5 per plate in 3.5 cm diameter cell culture dishes and 10 x 10^6 cells per well in 96-well cell culture plates and allowed to adhere for 24 h prior to treatment. Cells were treated with varying concentrations (10, 25, 50, 100, & 200 µg/mL) of AuNPs and incubated for 24h. After 24h, treated cells were exposed to visible light diode laser (525 nm) at fluency of 10J/cm^2 for 5 mins.

2.4 Morphological analysis

Cellular morphological changes in MCF-7 cells were evaluated 24 hours post treatment using inverted brightfield microscope (Olympus CKX41, Wirsam Scientific). Each treatment group, including cells exposed to AuNPs, laser irradiation, PTT (AuNPs + laser), and untreated controls, was observed to access alterations in cell structure, integrity, and density. Morphological features such as cell shrinkage, rounding, detachment and membrane blebbing were recorded as indicators of photothermal-induced cytotoxicity.

2.5 Cytotoxicity and cell proliferation analysis

Cytotoxicity was evaluated using the MTT assay (Roche Cell Proliferation Kit). 10µL of MTT reagent was added to each well containing 90µL cell culture medium, and the plate was incubated for 3 hours at 37°C. After incubation, 100 µL of solubilization buffer was added, and the plate was left overnight to ensure complete formazan dissolution. Absorbance was recorded at 570 nm using the VICTOR Nivo multimode microplate reader. Cellular proliferation was assessed using the CellTiter-Glo Luminescent Cell Viability Assay, which quantifies intracellular ATP as an indicator of metabolically active cells. Following treatment, the reagent was

added to each well in accordance with the manufacture's protocol. Luminescence was measured using the same multimode microplate reader.

2.6 Statistical analysis

All experiments were conducted in triplicate and independently repeated three times. Results were expressed as mean and standard error of the mean, comparisons between untreated and treated groups were performed using Dunnett test. Statistical significance was evaluated at a 95% confidence interval. Data analysis was conducted using SigmaPlot software. Significance levels were indicated as $p < 0.05$ (*), $p < 0.01$ (**) or $p < 0.001$ (***).

3 Results

3.1 Characterization of gold nanoparticles

3.1.1 UV-vis spectrometry

UV-vis spectrometry was used to confirm successful green synthesis of AuNPs and the interaction between K. porphyrantha and gold ions. As shown in Figure 1 below, the UV-vis the UV-vis spectrum of the plant extract displayed a strong absorbance peak at around 520 nm, which is typical for spherical AuNPs and confirms their formation. The spectrum of the reaction mixture of both the plant extract and SPR peak at 520 nm indicates the successful reduction of gold ions and capping of the nanoparticles by phytochemicals present in the extract.

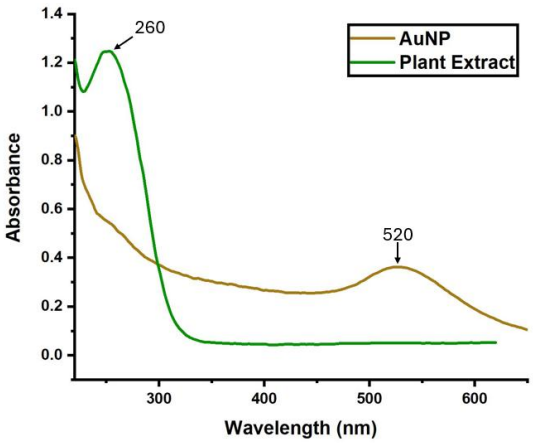

Figure 1: UV-vis absorption spectra of *Kniphophia porphyrantha* plant extract (260 nm) and green synthesized gold nanoparticles (520 nm).

3.1.2 Size distribution and Zeta potential

The size and surface characteristics of the green-synthesized AuNPs were assessed using DLS and Zeta potential analysis. As illustrated in Figure 2 (*left*), the DLS results revealed a dominant particle size distribution around 97.47 nm, contributing to over 93% of the intensity, with a smaller secondary population at approximately 12.48 nm. The Z-average diameter was determined to be 62.14 nm with a polydispersity index (PDI) of 0.348, suggesting moderate polydispersity.

Zeta potential measurements (Figure 2 (*right*)) indicated a mean surface charge of -15.9 mV, suggesting moderate colloidal stability due to electrostatic repulsion, essential for preventing aggregation in aqueous media.

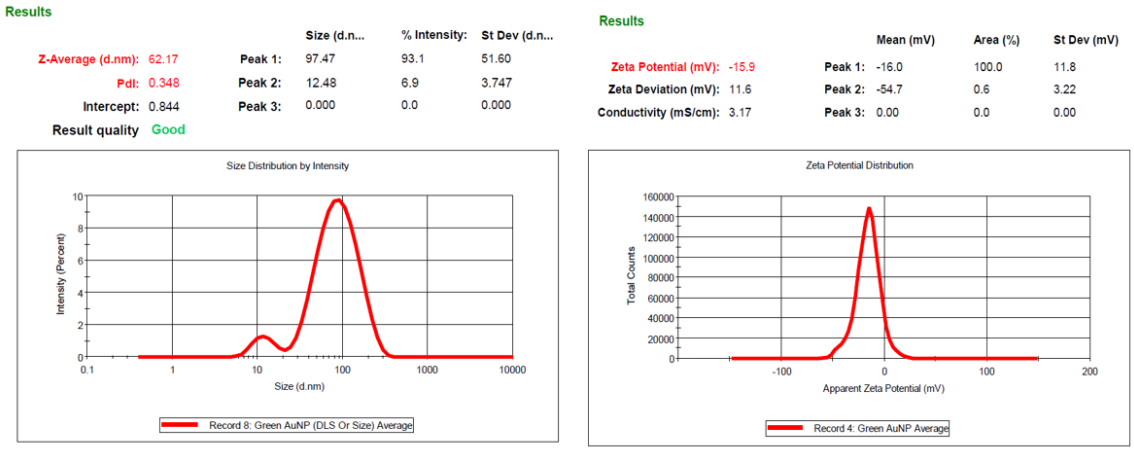

Figure 2: (*left*) Size distribution by intensity shows a dominant population around 97 nm and a smaller population near 12 nm. The Z-average diameter was 62.17 nm with a PDI of 0.3488. (*right*) Zeta potential distribution showing a major peak at -15.9 mV, indication colloidal stability.

3.2 Morphological analysis

The observed morphological changes in MCF-7 cells following treatment with green-synthesized AuNPs and PTT (Figure 3) included cell shrinkage, rounding of cells, detachment from the culture plate, and vesicle formation when compared to the untreated group.

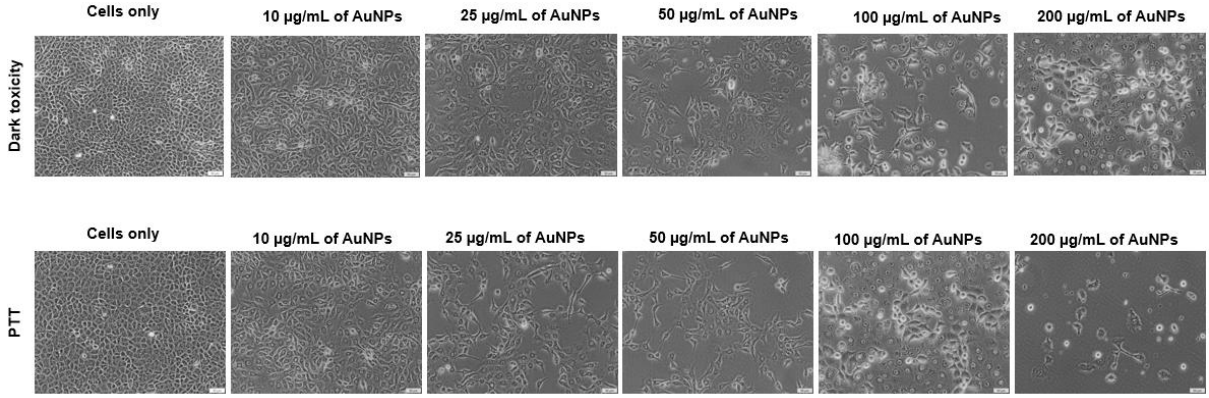

Figure 3: Inverted microscopy images showing the photothermal effects of green-synthesized AuNPs on MCF-7 cells under dark conditions (top row) and following PTT (bottom row). Cells were treated with increasing concentrations of AuNPs (10, 25, 50, 100, & 200 µg/mL). In both conditions, dose-dependent morphological changes were observed, including cell shrinkage, rounding of cells, detachment from the culture plate, and vesicle formation.

3.3 Cytotoxicity and cell proliferation analysis

3.3.1 MTT cell viability analysis

MTT analysis (Figure 4) demonstrated a significant PTT of green-synthesized AuNPs. Cells exposed to laser irradiation alone showed no noticeable decrease in cell viability compared to untreated cells only, indicating minimal toxicity. However, a significant dose-dependent decrease in cell viability was observed in cells treated with varying concentrations of AuNPs. On further analysis, following laser irradiation of these groups, cell viability significantly declined in a dose-dependent manner, with the most significant decrease in cell viability at 200 µg/mL.

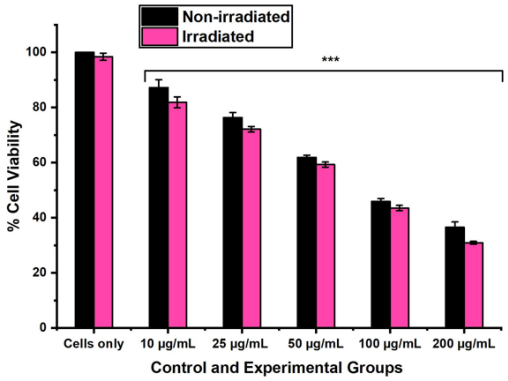

Figure 4: Quantitative MTT assay showing percentage cell viability of MCF-7 breast cancer cells treated with increasing concentrations (10, 25, 50, 100, 200 µg/mL) of green-synthesized AuNPs under dark (black) and PTT (pink) conditions. A significant dose-dependent reduction in cell viability was observed in both conditions, with increased cytotoxicity in PTT groups, confirming photothermal enhancement. *($p < 0.05$ (*), $p < 0.01$ (**) or $p < 0.001$ (***)).*

3.3.2 ATP cell proliferation analysis

ATP analysis (Figure 5) further confirmed the photothermal-induced inhibition of cell viability and proliferation. In non-irradiated cells, a steady decline of ATP levels was recorded across all concentrations, suggesting mitochondrial stress even without light activation. However, irradiated groups showed a greater decrease in ATP luminescence, with the strongest inhibitory effect observed at 200 µg/mL.

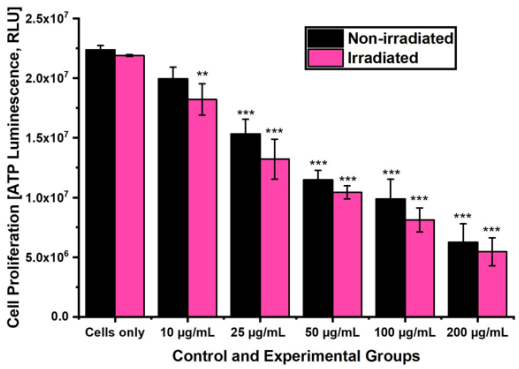

Figure 5: Quantitative ATP assay showing percentage cell proliferation of MCF-7 breast cancer cells treated with increasing concentrations (10, 25, 50, 100, 200 /mL) of green-synthesized AuNPs under dark (black) and PTT (pink) conditions. A significant decrease in cell proliferation was observed in a dose-dependent manner in both conditions, with a higher decline in PTT groups, confirming photothermal enhancement. *($p < 0.05$ (*), $p < 0.01$ (**) or $p < 0.001$ (***)).*

4 Discussion

Green-synthesized AuNPs have shown promising anticancer effects in several studies [8], including against breast cancer cell lines [9]. In this study, AuNPs synthesized using *K. porphyrantha* extract displayed a SPR peak at approximately 525 nm. Confirming their suitability for laser-induced PTT. DLS analysis revealed an average size of 62 nm and a zeta potential of -15.9, indicating moderate stability, dispersion, and efficient cellular uptake. The demonstrated moderate cytotoxicity at concentrations above 50 µg/mL in non-irradiated MCF-7 cells, with increased effects observed under photothermal conditions at 25 µg/mL. This suggests that that AuNPs are cytotoxic on their own. Morphological analysis (Figure 3) confirmed apoptotic features, such as membrane blebbing, rounding of cells, and cell detachment. Following laser irradiation, cell viability decreased significantly, with 60-70% cell death observed at 100-200 µg/mL (Figure 4). Increased levels of ATP depletion

(Figure 5) suggest mitochondrial damage and metabolic shutdown. These results are consistent with cell death pathways such as apoptosis and necrosis [10]. Laser activation likely intensifies cellular stress through localized heating, disruption of protein function and cellular repair mechanisms, mitochondrial impairment, and cell membrane destabilization. In particular, thermal stress compromises membrane integrity, increasing permeability ad facilitating deeper nanoparticles uptake and intracellular damage [3]. Notably, no other studies have reported the use of *K. porphyrantha* extract for the green synthesis of AuNPs, highlighting its novelty and potential in cancer nanomedicine.

5 Conclusion

Green synthesized AuNPs from *K. porphyrantha* showed strong photothermal effects against MCF-7 breast cancer cells. Laser irradiation increased their cytotoxicity, reducing cell viability and ATP levels in a dose-dependent manner. This eco friendly approach shows promise as selective and minimal invasive cancer therapy, supporting its potential for future clinical application.

Acknowledgements

The authors sincerely thank the South African Research Chairs initiative of the Department of Science and Technology and the National Research Foundation (NRF) of South Africa (Grant No. 98337), South African Medical Research Council (Grant No. SAMRC EIP007/2021), South African Development Community (SADC), as well as grants received from the NRF Research Development Grants for Y-Rated Researchers (Grant No. 137788), Council for Scientific Industrial Research (CSIR)-National Laser Centre (NLC), African Laser Centre (ALC), and University Research Committee (URC).

References

[1] F. Bray *et al.*, "Global cancer statistics 2022: GLOBOCAN estimates of incidence and mortality worldwide for 36 cancers in 185 countries," (in eng), *CA Cancer J Clin,* vol. 74, no. 3, pp. 229-263, May-Jun 2024, doi: 10.3322/caac.21834.

[2] J. Ferlay *et al.* "Global Cancer Observatory: Cancer Today." International Agency for Research on Cancer. https://gco.iarc.who.int/today (accessed 11 December 2024, 2024).

[3] A. H. Faid, S. A. Shouman, N. A. Thabet, Y. A. Badr, and M. A. Sliem, "Laser Enhanced Combinatorial Chemo-photothermal Therapy of Green Synthesis Gold Nanoparticles Loaded with 6Mercaptopurine on Breast Cancer Model," *Journal of Pharmaceutical Innovation,* vol. 18, no. 1, pp. 144-148, 2023/03/01 2023, doi: 10.1007/s12247-022-09626-0.

[4] R. Chaudhari, V. Patel, and A. Kumar, "Cutting-edge approaches for targeted drug delivery in breast cancer: beyond conventional therapies," *Nanoscale Advances,* 10.1039/D4NA00086B vol. 6, no. 9, pp. 2270-2286, 2024, doi: 10.1039/D4NA00086B.

[5] M. Broadbent, S. J. Chadwick, M. Brust, and M. Volk, "Gold Nanoparticles for Photothermal and Photodynamic Therapy," *ACS Omega,* vol. 9, no. 44, pp. 44846-44859, 2024/11/05 2024, doi: 10.1021/acsomega.4c08797.

[6] G. Nigussie, M. Tegegn, D. Abeje, and H. Melak, "A comprehensive review of the ethnomedicine, phytochemistry, pharmacological activities of the genus Kniphofia," (in eng), *Pharm Biol,* vol. 60, no. 1, pp. 1177-1189, Dec 2022, doi: 10.1080/13880209.2022.2085753.

[7] A. Ullah *et al.*, "Important Flavonoids and Their Role as a Therapeutic Agent," (in eng), *Molecules,* vol. 25, no. 22, Nov 11 2020, doi: 10.3390/molecules25225243.

[8] S. Sargazi *et al.*, "Application of Green Gold Nanoparticles in Cancer Therapy and Diagnosis," *Nanomaterials,* vol. 12, no. 7, p. 1102, 2022. [Online]. Available: https://www.mdpi.com/2079-4991/12/7/1102.

[9] A. K. Singh *et al.*, "Green synthesis of gold nanoparticles from Dunaliella salina, its characterization and in vitro anticancer activity on breast cancer cell line," *Journal of Drug Delivery Science and Technology,* vol. 51, pp. 164-176, 2019/06/01/ 2019, doi: https://doi.org/10.1016/j.jddst.2019.02.023.

[10] S. L. Fink and B. T. Cookson, "Apoptosis, pyroptosis, and necrosis: mechanistic description of dead and dying eukaryotic cells," (in eng), *Infect Immun,* vol. 73, no. 4, pp. 1907-16, Apr 2005, doi: 10.1128/iai.73.4.1907-1916.2005.